



ELSEVIER

Available online at www.sciencedirect.com

SCIENCE @ DIRECT®

Applied Surface Science 219 (2003) 228–237

applied
surface science

www.elsevier.com/locate/apsusc

Properties of fluorinated amorphous diamond like carbon films by PECVD

G.Q. Yu^{*}, B.K. Tay, Z. Sun, L.K. Pan

School of Electrical and Electronic Engineering, Nanyang Technological University, Nanyang Avenue, Singapore 639798, Singapore

Received 12 December 2002; received in revised form 29 April 2003; accepted 29 April 2003

Abstract

Fluorinated amorphous diamond-like carbon films (a-DLC:F) were prepared on room-temperature Si(1 0 0) substrates using radio frequency plasma enhance chemical vapor deposition (rf PECVD) by varying the ratio of carbon tetrafluoride and methane ($\text{CF}_4:\text{CH}_4$). The films formed were investigated in terms of the surface morphology, chemical composition, microstructure, mechanical properties, and surface free energy by means of atomic force microscopy (AFM), X-ray photoelectron spectrum (XPS), micro-scratch test, nano-indenter test and contact angle measurement. Emphasis was placed on investigation of the factors affecting the film surface energy, which was calculated from three methods (the harmonic mean equation, the geometric mean equation and acid–base equation). It was observed that with increasing $\text{CF}_4:\text{CH}_4$, the roughness and F content of the a-DLC:F films increased while the hardness, Young's modulus and surface energy decreased. The films also became more graphitized. The reduction of the film surface energy with varying F content is believed to be mainly due to the change of bonds in the film, i.e. the decrease of $-\text{C}-\text{CF}$ bond and corresponding increase of $-\text{CF}$, $-\text{CF}_2$. The roles of the roughness and the microstructure in affecting the film surface energy were negligible.

© 2003 Elsevier Science B.V. All rights reserved.

PACS: 68.35.Md; 81.15.Gh; 82.80.Pv

Keywords: Fluorinated amorphous diamond-like carbon films; X-ray photoelectron spectrum; Surface free energy

1. Introduction

Diamond-like carbon (DLC) films are known for their high hardness, wear resistance, chemical inertness, and low friction coefficients [1]. The properties of DLC may be modified by incorporation of dopants [2], such as silicon, fluorine, nitrogen, oxygen and various metals. It has been reported that incorporation of fluorine into DLC film will greatly reduce its

surface free energy but almost keep DLC-behavior [3]. The non-wetting behavior combined with DLC superior properties allows numerous practical applications in non-stick kitchenware and protective coatings for optics. The surface free energy of materials is a characteristic factor, which affects the surface properties and interfacial interactions such as adsorption, wetting and adhesion, etc.

In this work, radio frequency plasma enhanced chemical vapor deposition (rf PECVD) was employed to prepare fluorinated amorphous DLC film (thereafter denoted as a-DLC:F) using carbon tetrafluoride (CF_4) and methane (CH_4) as precursors. The deposition was

^{*} Corresponding author. Tel.: +65-6790-5454;
fax: +65-6793-3318.
E-mail address: egqyu@ntu.edu.sg (G.Q. Yu).

performed as a function of $\text{CF}_4:\text{CH}_4$ ratio at rf power of 60 W. The films properties were investigated by means of contact angle measurement, atomic force microscopy (AFM), X-ray photoelectron spectroscopy (XPS), Raman spectroscopy, scratch test and nano-indenter. The emphasis studied was focused to investigate the factors affecting the film surface energy.

2. Experimental details

2.1. Film preparation

The experimental setup, capacitively coupled radio frequency (13.56 MHz) plasma enhanced chemical vapor deposition (rf PECVD) was schematically given in Fig. 1, where its configuration is asymmetrical. As such, self-bias will be produced on substrate during the deposition. This self-bias originates from the large difference of motion speed between electrons and ions in plasma [4], and depends on process parameters, such as rf power applied, as shown in Fig. 2. After being ultrasonically cleaned in acetone, methanol and de-ionized water in sequence, Si(1 0 0) substrates were placed on the cathode electrode kept at room-tempera-

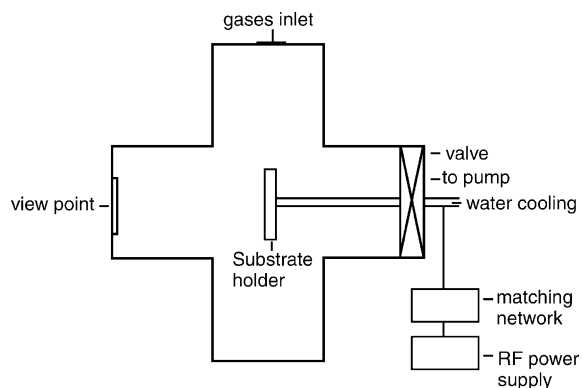


Fig. 1. Schematic diagram of our experimental setup.

ture by cooling water. The base vacuum in the chamber is $\sim 10^{-6}$ Torr. Before deposition, the substrates were in situ sputter cleaned for 10 min in argon plasma operated at 100 W. High-purity CH_4 and CF_4 were led into chamber as gas precursors. A very thin carbon interlayer was first deposited to improve the overall adhesion, and then a-DLC:F films were deposited at varying $\text{CF}_4:\text{CH}_4$ flow rate ratio (referred to as $\text{CF}_4:\text{CH}_4$) and 60 W power. A DLC film deposited by the same setup was used as a reference sample. During deposition, the process pressure was fixed at 50 mTorr.

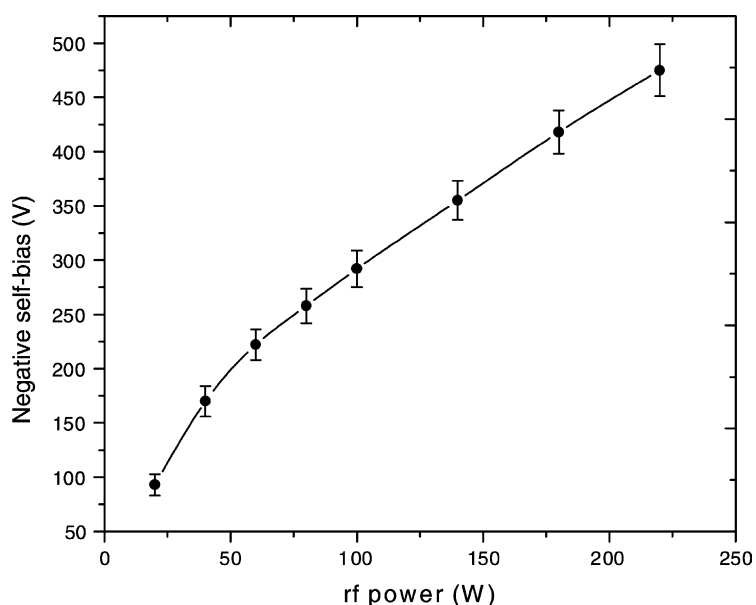


Fig. 2. Relationship between self-bias and rf power.

2.2. Surface energy calculation

The surface free energy of the samples is generally obtained from measuring contact angle formed when liquid drops on the sample surface. The relationship between surface energy of the sample (γ_s) and the contact angle (θ) is universally described by the Young equation [5],

$$\gamma_s = \gamma_L \cos \theta + \gamma_{LS}$$

where γ_L is the known surface energy of the testing liquid, γ_{LS} the unknown interfacial energy of the film/liquid. To eliminate γ_{LS} from the equation, many methods have been developed based on consideration of the intermolecular forces. Among all, three methods [6–8] are often used, namely the harmonic mean equation (Eq. (1)), the geometric mean equation (Eq. (2)) and acid–base equation (Eq. (3)). They are expressed, respectively, as follows,

$$\gamma_{LS} = \gamma_s + \gamma_L - 4 \left(\frac{\gamma_s^d \gamma_L^d}{\gamma_s^d \gamma_L^d} + \frac{\gamma_s^p \gamma_L^p}{\gamma_s^p \gamma_L^p} \right) \quad (1)$$

$$\gamma_{LS} = \gamma_s + \gamma_L - 2 \left(\sqrt{\gamma_s^d \gamma_L^d} + \sqrt{\gamma_s^p \gamma_L^p} \right) \quad (2)$$

$$\gamma_{LS} = \gamma_s + \gamma_L - 2 \left(\sqrt{\gamma_s^{LW} \gamma_L^{LW}} + \sqrt{\gamma_s^+ \gamma_L^-} + \sqrt{\gamma_s^- \gamma_L^+} \right) \quad (3)$$

where γ with superscript d and p means a dispersion component and a polar component, γ with superscript LW, (+) and (–) stands for a Lifshitz–van der Waals component, Lewis acid component and Lewis base component. Three liquids with different polarity, de-ionized water, methylene iodide (CH_2I_2) and formamide, were applied for the measurement. The contact angle was averaged over four data obtained from different spots on the samples for each liquid. Comparison on the surface energy calculated from the above methods was also performed.

It should be pointed out that another surface energy, critical surface energy (γ_c) is often mentioned elsewhere. This critical surface energy is introduced by Zisman [9], and is the surface energy of a reference liquid which fully wets the sample surface, i.e. $\gamma_c = \gamma_L = \gamma_s$ at $\theta = 90^\circ$. In this work, this value was not given.

2.3. Other characterizations

The surface morphology of the films was observed over $1 \mu\text{m} \times 1 \mu\text{m}$ by a scanning atomic force microscope (AFM, Nanoscope IIIa) with a tapping mode. The chemical composition and bonding states of the films were characterized by X-ray photoelectron spectroscopy (XPS) with Al K α line (1486.6 eV) as the exciting source. In this characterization, the system was calibrated by the binding energy (~ 284.7 eV) of C 1s and all samples were analyzed without surface etching. A micro-Raman spectroscopy (Renishaw 1000) with 514.5 nm Ar⁺ laser was used to study the film microstructure, where the laser output power used was ~ 2 mW. The adhesion property was analyzed by micro-scratch test. Scratch test parameters used were as follows: progressive type, a maximum load of 25 N, loading rate of 4 N/min, the scratch length of 5 mm Rockwell-type diamond indenter with 200 μm radius. The hardness (H) and Young's modulus (E) were characterized by a nano-indenter (nano-indenter II, nano-instruments), where the continuous stiffness option was used and the maximum load was 10 mN.

3. Results

3.1. Surface morphology

Fig. 3 gave a typical AFM image of the a-DLC:F films. The films deposited were all uniform and smooth. Compared with DLC reference sample (0.17 nm), the a-DLC:F films exhibited more rougher surface. The surface roughness also increased with $\text{CF}_4:\text{CH}_4$, from 0.23 nm at 1:4–0.28 nm at 4:1, as shown in Fig. 4. The increase was possibly caused by fluorine preferential etching of the films since the films were not ideally isotropic. In addition, the variation of the roughness with the ratio seemed not monotonous.

3.2. Chemical compositions and bonding states

Fig. 5 showed the C 1s local XPS spectrum for the film deposited at 1:1. It was well decomposed into four peaks, which centered at ~ 284.9 , ~ 287.4 , ~ 289.8 and ~ 292.3 eV, respectively. Due to surface contamination

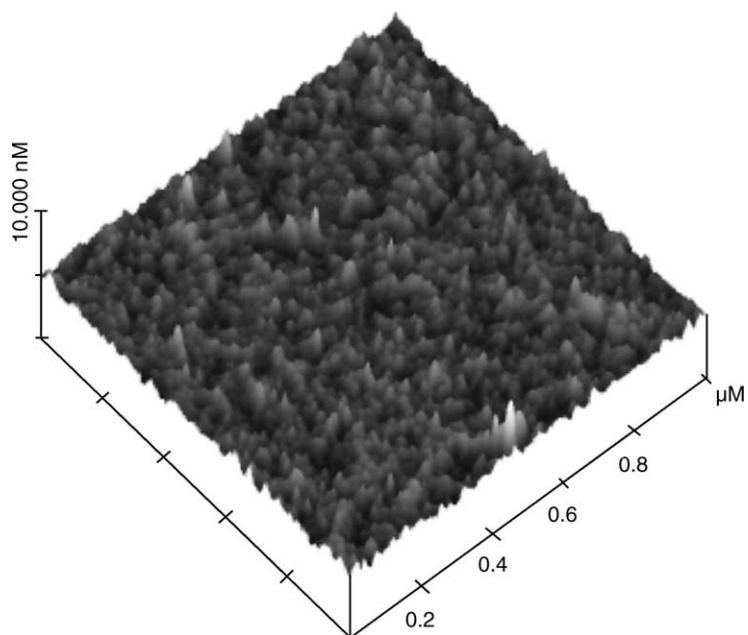


Fig. 3. A typical AFM image of the film (1:1).

and charging effect during XPS analysis, it is very complex and also still controversial to identify these peaks. According to Touhara and Okino [10], the peak at 285 eV was assigned to the carbon atoms with the

mixed bonded structures of sp^2 and sp^3 configurations, and the peak at 287 eV was due to the carbon atoms bonded to oxygen. In addition, the peaks with 289 and 291 eV were ascribed to CF bonds and CF_2 bonds,

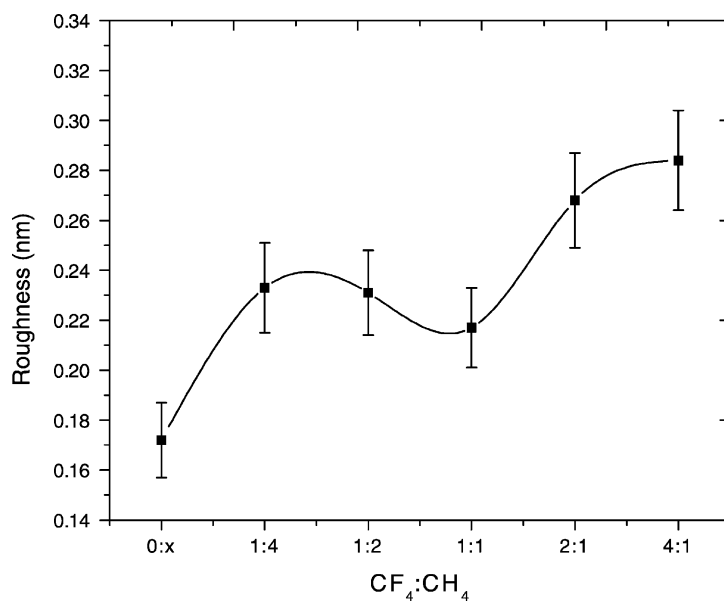


Fig. 4. The film roughness dependent of $CF_4:CH_4$.

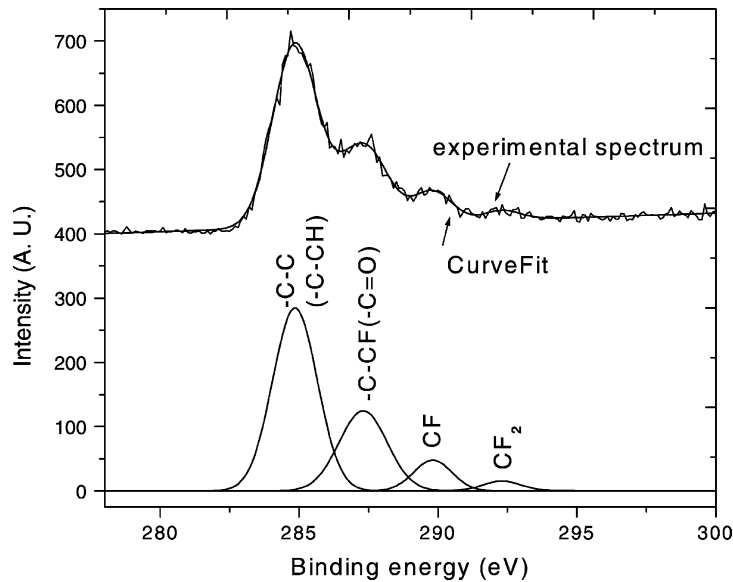


Fig. 5. C 1s XPS spectrum of the film (1:1).

respectively. The peak at ~ 292 eV was not reported. In other references [11–14], assignment was made between binding energy and structural unit as: $-C-CH$ (284.6 eV), $-C-CF$ (287.4 eV), $-CF$ (289.5 eV), $-CF_2$ (292 eV), $-CF_3$ (294 eV). Based on the above data and the fact that a small amount of oxygen occurs on the films surface and hydrogen always occurs in the PECVD-deposited films as reflected in the Raman spectrum below, assignment is done as follows: $-C-C$ and $-C-CH$ (284.9 eV), $-C-CF$ and $-C=O$ (287.4 eV), $-CF$ (289.8 eV) and $-CF_2$ (292.3 eV), where the fraction of $-C-CH$ and $-C=O$ should be much lower than that of $-C-C$ and $-C-CF$, respectively. On the other hand, F atomic concentration can be obtained by the following equation:

$$\text{atomic concentration (\%)} = \frac{A_i/S_i}{\sum_i (A_i/S_i)}$$

where subscript is film element, A and S is the peak area and sensitivity factor of the element ($S = 0.78$, 1.00 for C 1s and F 1s [10]). Similarly, the bond concentration was also done according to the relevant peak area divided by the sum of all the peaks area. Their concentrations were presented in Fig. 6, with varying $CF_4:CH_4$. It was observed that F was incorporated into the films with addition of CF_4 , and then increased correspondingly with $CF_4:CH_4$. At $CF_4:CH_4$

of 1:4, F incorporated existed primarily in the form of CF bond state ($-C-CF$ and $-CF$). The amount of $-C-CF$ was greater than that of $-CF$. As $CF_4:CH_4$ increased up to 4:1, the former content decreased while the latter concentration increased relatively slightly. What's more, when $CF_4:CH_4$ increased to 1:1, another bonding state, $C-F_2$ appeared in the films. Afterwards, $C-F_2$ content gradually increased with increasing $CF_4:CH_4$.

3.3. Microstructure

The microstructure of the a-DLC:F film was very similar to that of DLC (Fig. 7), where G-band (“graphite”, ~ 1540 cm^{-1}) and D-band (“disorder”, ~ 1340 cm^{-1}) were obviously observed after fitting. The G-band originates from the symmetric E2g vibrational mode in graphite-like materials, while the D-band arises from the limitations in the graphite domain size induced by grain boundaries or imperfections [15], e.g. sp^3 carbon, or other impurities. Quantitative analysis (Fig. 8) revealed that the intensity ratio of D- and G-band (I_D/I_G) increased, and G-band shifted upward with increasing $CF_4:CH_4$, which were due to an increased number of sp^2 bonds and the formation of sp^2 clusters in the amorphous network, i.e. rings or chains [16]. This result indicated the films became

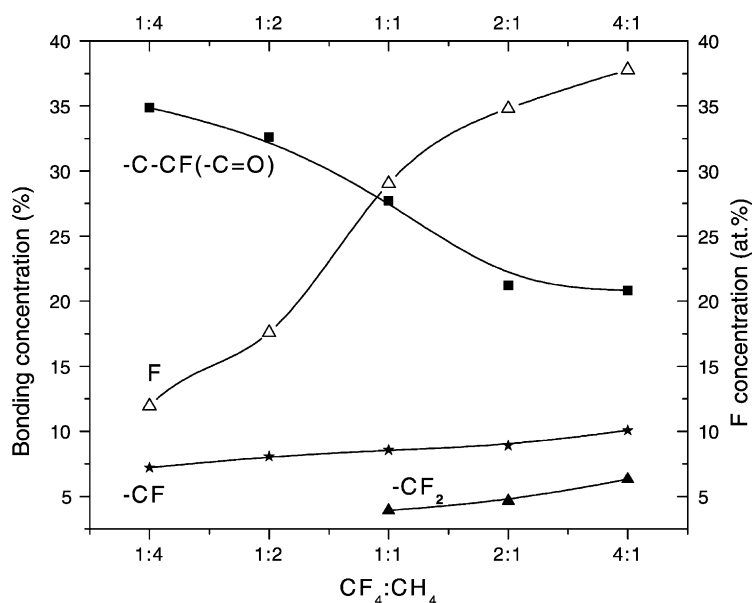


Fig. 6. Concentrations of F and bonds of films at different $CF_4:CH_4$.

more graphitic with the increase in F content. It was also found that photoluminescence (PL) background appeared in Raman spectra, and decreased with more addition of CF_4 . The PL is generally believed to originate from hydrogen (H) or be due to that film is polymer-like as confirmed in carbon nitride film

[17–19]. In our case, the films deposited are diamond-like carbon as disclosed later. It is therefore concluded the PL here is ascribed to H atoms in the films, where some H atoms are replaced by F atoms due to F incorporation and the PL intensity is reduced correspondingly. It should be here pointed out that, to some

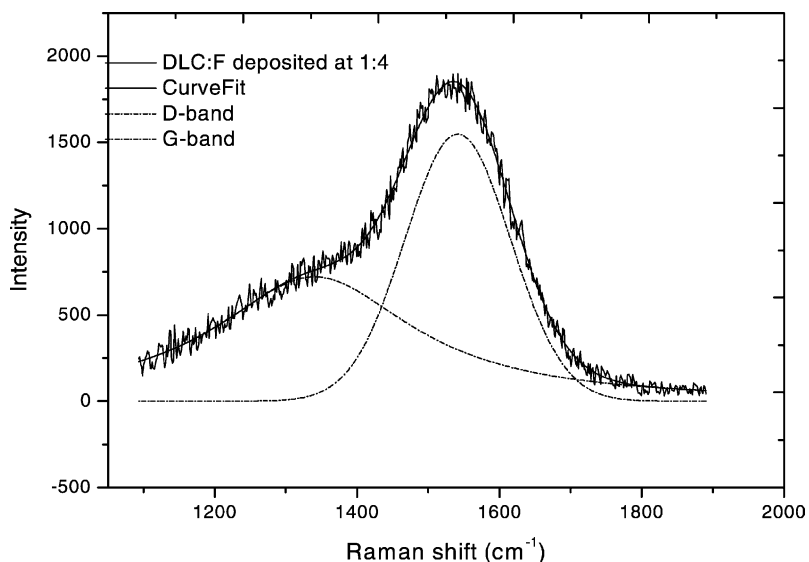


Fig. 7. A typical Raman spectrum of a-DLC:F film (1:4).

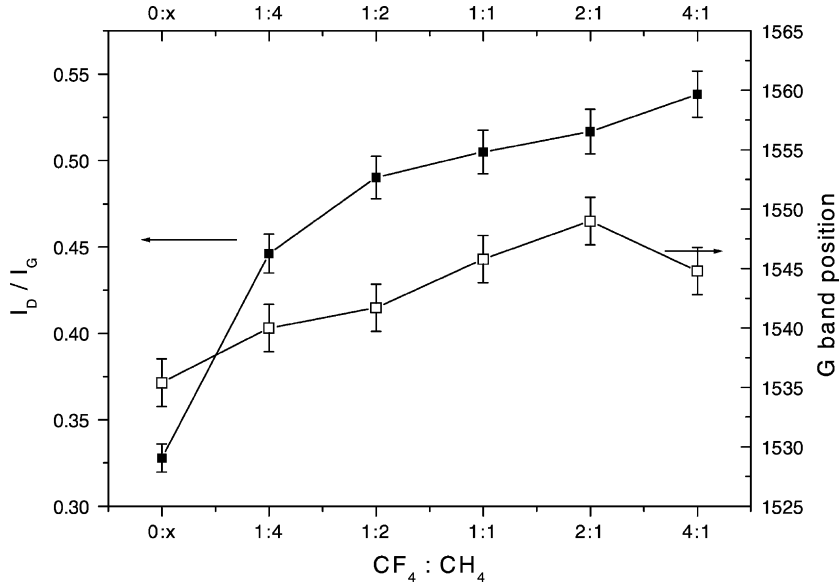


Fig. 8. Dependence of I_D/I_G and G-band peak position on $CF_4:CH_4$.

extent, the role of F is similar to that of N in carbon nitride film, where C–H content also decreases with more incorporation of N, as evidenced by FTIR analysis [19].

3.4. Mechanical properties

Scratch test disclosed the a-DLC:F films were all well adhesive to the substrate (not shown). The

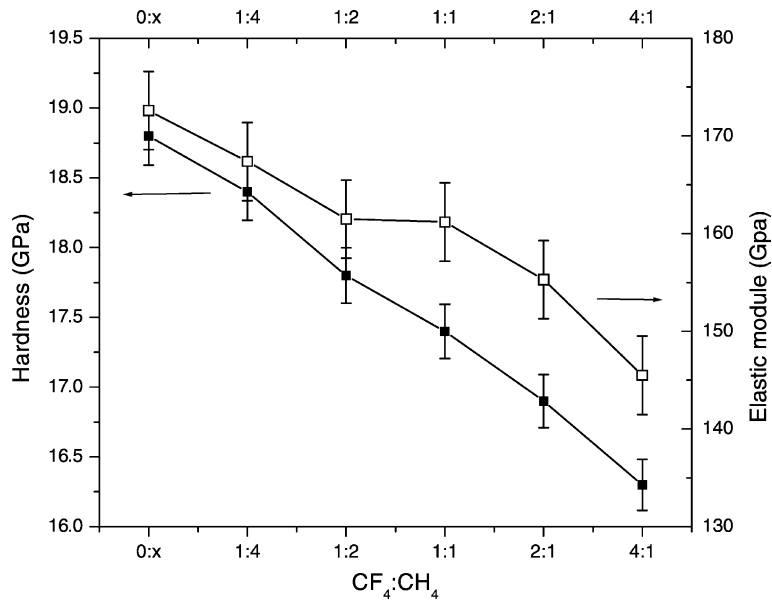


Fig. 9. Dependence of the film hardness and modulus on $CF_4:CH_4$.

hardness (H) and Young's modulus (E) can be calculated from the indentation load-displacement data [20]. It was drawn that the film hardness and modulus both decreased with increasing $\text{CF}_4:\text{CH}_4$ (Fig. 9). As shown, with the introduction of CF_4 gas, the film hardness and modulus slightly dropped compared with that of DLC reference sample. When $\text{CF}_4:\text{CH}_4$ increased, they further decreased. The lowest hardness was ~ 16 GPa larger than that of Si substrate (~ 12 GPa). This hardness feature of the films is guaranteed by the above-mentioned self-bias produced on the substrate, which increases the bombarding energy of deposited species and therefore results in the formation of DLC films [21]. The decrease in the film hardness is believed to be partly due to change in the microstructure as concluded from Raman analysis,

i.e. more graphitized with more incorporation of F into the films. Another possible cause is the reduction in the internal stress of the films induced by F incorporation into the films.

3.5. Surface free energy

Fig. 10 showed the variation of the film surface energy with varying $\text{CF}_4:\text{CH}_4$. From (a), after introduction of CF_4 at 1:4, the surface energy was sharply reduced compared with that of DLC reference sample, suggesting something like chemical composition altered in the films. The reduction extent calculated from the geometric mean method was more than those from the other two. On the other hand, the reduction rate did not vary until $\text{CF}_4:\text{CH}_4$ reached 1:2. After that,

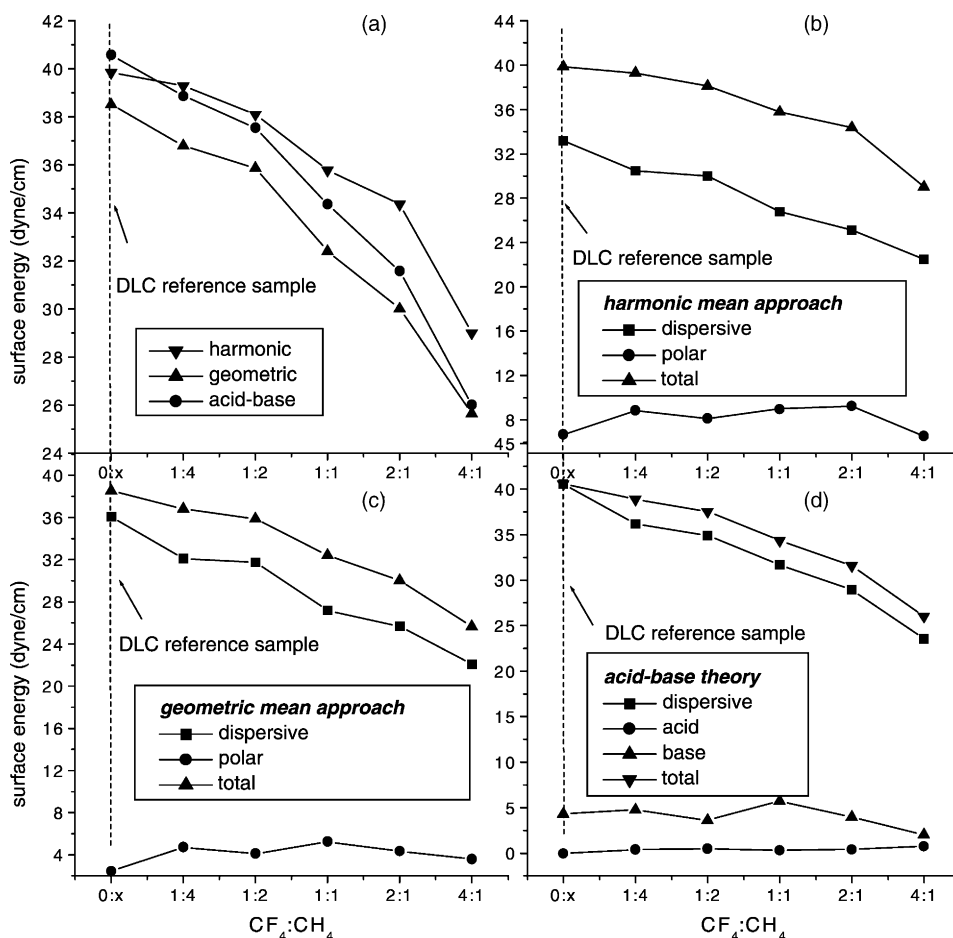


Fig. 10. Surface energy of the films deposited at the different $\text{CF}_4:\text{CH}_4$.

the reduction rate increased. As $\text{CF}_4:\text{CH}_4$ increased to 2:1, the surface energy seemed to drop most quickly. The change in the reduction rate was very similar for all the methods. From (b) and (c), it was also concluded that the reduction in the surface energy was largely ascribed to the decrease in the dispersion component, which was not dependent on the calculation approaches.

4. Discussion

In general, the surface roughness affects the measured contact angle and therefore the surface energy. According to Neumann [22], a model similar to that for heterogeneous solid surface can be developed in order to account for surface irregularities, being given by Wenzel's equation,

$$\cos \theta = r \cos \theta_0$$

where θ is the measured contact angle, θ_0 is the thermodynamical value for the smooth surface, and r quantifies the surface roughness (ratio of the real area of the surface to the apparent area of the geometrical interface). Clearly, more rougher the contact surface (larger r) is, more smaller is the observed contact angle (larger surface energy). However, as concluded from the AFM test (Fig. 4) and the contact angle measurement (Fig. 10), with increasing $\text{CF}_4:\text{CH}_4$, the film surface roughness increased while the surface energy decreased. Therefore, the relationship between the roughness and the measured contact angle does not follow the above equation. As such, it is concluded that the roughness plays a negligible role on the surface energy. This may be ascribed to the fact the surface roughness is so small. A similar result for other materials was reported elsewhere [23–25].

The effect of F content in the films on the surface energy is very noticeable (Figs. 6 and 10). As pointed out above, besides a small fraction of $-\text{C}-\text{H}$ and $-\text{C}=\text{O}$ bonds, there are $-\text{C}-\text{C}$, $-\text{C}-\text{CF}$, $-\text{CF}$ and $-\text{CF}_2$ bonds in the films, where $-\text{C}-\text{C}$ bond is the backbone of DLC film. The bonding states and their contents changed with increasing F content. With increasing F content up to $\sim 37\%$, $-\text{C}-\text{CF}$ bond content decreased and $-\text{CF}$ increased, while the surface energy decreased. Especially, at F content of $\sim 30\%$, $-\text{CF}_2$ appeared

and thereafter also increased with F content. The bonds associated with F have a corresponding trend as the surface energy does with increasing F content. It is thus concluded that the reduction in the surface energy is mainly caused by the decrease of $-\text{C}-\text{CF}$ bond and the increase of $-\text{CF}$ and $-\text{CF}_2$ bonds. The introduction and increase of $-\text{CF}_2$ is maybe responsible for the accelerating decrease in the surface energy since $-\text{CF}_2$ is a basic unit of PTFE, which is a simple linear $\text{C}-\text{C}$ backbone with two F atoms on each C atom and possesses the lowest surface energy.

The effect of the film microstructure on the surface energy was very negligible. The film became more graphitized as more F was incorporated. This graphitization should not account for the reduction of the surface energy.

It is well known that surface energy originates from the unbalance of the force between atoms or molecules inside and interface. Generally, the polar component results from three different intermolecular forces due to permanent and induced dipoles and hydrogen bonds, whereas the dispersion component arises from instantaneous dipole moments [23]. So, the variation of $-\text{C}-\text{CF}$, $-\text{CF}$ and $-\text{CF}_2$ bonds mainly lowered the dispersion component, and therefore reduced the surface energy of the film significantly.

5. Conclusions

Fluorinated amorphous diamond-like carbon films (a-DLC:F) were prepared on room-temperature Si(1 0 0) substrates by rf PECVD. The films were investigated in terms of the surface morphology, chemical composition, microstructure, mechanical properties, and surface free energy by means of atomic force microscopy (AFM), X-ray photoelectron spectrum (XPS), micro-scratch test, nano-indenter test and contact angle measurement. It was observed that with increasing $\text{CF}_4:\text{CH}_4$, the roughness, F content of the a-DLC:F films increased while the hardness, Young's modulus and surface energy decreased. The films also became more graphitized. The reduction of the surface energy with varying F content is believed to be mainly due to the change of bonds in the film, i.e., $-\text{C}-\text{CF}$ bond decreased and $-\text{CF}$, $-\text{CF}_2$ increased. The roughness and the microstructure played negligible roles in affecting the film surface energy.

References

- [1] A. Grill, *Diamond Relat. Mater.* 8 (1999) 428.
- [2] M. Grischke, K. Bewilogua, K. Trojan, H. Dimigen, *Surf. Coat. Technol.* 74/75 (1995) 739.
- [3] R. Memming, *Thin Solid Films* 143 (1986) 279.
- [4] B. Chapman, *Glow discharge processes: sputtering and plasma etching*, Wiley, New York, 1980.
- [5] T. Young, *Philos. Trans. R. Soc. Lond.* 9 (1805) 255.
- [6] S. Wu, *J. Polym. Sci.: Part C* 34 (1971) 19.
- [7] D.K. Owens, R.C. Wendt, *J. Appl. Polym. Sci.* 13 (1969) 1741.
- [8] F.M. Fowkes, *J. Adhes. Sci. Technol.* 1 (1987) 7.
- [9] W.A. Zisman, *Ind. Eng. Chem.* 55 (1963) 19.
- [10] H. Touhara, F. Okino, *Carbon* 38 (2000) 241.
- [11] A. Dilks, in: C.R. Brundle, A.D. Baker (Eds.), *Electron Spectroscopy*, Academic Press, London, 1981.
- [12] D.T. Clark, in: D. Briggs (Ed.), *Hand Book of X-ray Photoelectron Spectroscopy*, Heyden, London, 1978.
- [13] A. Dilks, E. Kay, *Macromolecules* 14 (1980) 855.
- [14] J.L. He, W.Z. Li, L.D. Wang, J. Wang, H.D. Li, *Nucl. Instr. Meth. Phys. Res. B* 135 (1998) 512.
- [15] N. Hellgren, M.P. Johansson, E. Broitman, L. Hultman, J.E. Sundren, *Phys. Rev. B* 59 (1999) 5162.
- [16] A.C. Ferrari, J. Robertson, *Phys. Rev. B* 61 (2000) 14095.
- [17] G.Q. Yu, S.H. Lee, J.J. Lee, *Diamond Relat. Mater.* 11 (2002) 1633.
- [18] N. Mutsukura, *Diamond Relat. Mater.* 10 (2001) 1152.
- [19] G.Q. Yu, S.H. Lee, D.G. Lee, H.D. Na, H.S. Park, J.J. Lee, *Surf. Coat. Technol.* 154 (2002) 68.
- [20] W.C. Oliver, G.M. Pharr, *J. Mater. Res.* 7 (1992) 1564.
- [21] C.A. Davis, G.A.J. Amaratunga, K.M. Knowles, *Phys. Rev. Lett.* 15 (1998) 3280.
- [22] A.W. Neumann, *Adv. Colloid Interface Sci.* 4 (1974) 328.
- [23] J.S. Chen, S.P. Lau, B.K. Tay, G.Y. Chen, Z. Sun, Y.Y. Tan, G. Tan, J.W. Chai, *J. Appl. Phys.* 89 (2001) 7814.
- [24] H.J. Busscher, A.W.J. van Pelt, P. de Boer, H.P. de Jong, J. Arends, *Colloids Surf.* 9 (1984) 319.
- [25] N. Sprang, D. Theirich, J. Engemann, *Surf. Coat. Technol.* 74/75 (1995) 689.